EARTHQUAKE ENGINEERING AND STRUCTURAL DYNAMICS, VOL. 26, 895–916 (1997)

STATISTICAL INSIGHT INTO CONSTANT-DUCTILITY DESIGN USING A NON-STATIONARY EARTHQUAKE GROUND MOTION MODEL

BOR-FENG PENG† AND JOEL P. CONTE*‡

Department of Civil Engineering, Rice University, P.O. Box 1892, Houston, TX 77251, U.S.A.

SUMMARY

A recently developed earthquake ground motion model non-stationary in both intensity and frequency content is validated at the inelastic Single-Degree-Of-Freedom (SDOF) structural response level. For the purpose of this study, the earthquake model is calibrated for two actual earthquake records. The objective of a constant (or target) displacement ductility used in conventional earthquake-resistant design is examined from the statistical viewpoint using this non-stationary earthquake model. The non-linear hysteretic structural behaviour is modelled using several idealized hysteretic SDOF structural models. Ensemble-average inelastic response spectra corresponding to various inelastic SDOF response (or damage) parameters and conditioned on a constant displacement ductility response are derived from the two identified stochastic ground motion models. The effects of the type of hysteretic behaviour, the structural parameters, the target displacement ductility factor, and the ground motion model on the statistics of the inelastic response parameters are thoroughly investigated. The results of this parametric study shed further light on the proper interpretation and use of inelastic response or damage parameters in earthquake-resistant design in order to achieve the desirable objective of 'constant-damage design'. © 1997 by John Wiley & Sons, Ltd.

Earthquake Engng. Struct. Dyn., **26**, 895–916 (1997)

No. of Figures: 12. No. of Tables: 0. No. of References: 30.

KEY WORDS: earthquake; non-stationary; inelastic response spectra; damage parameters; statistics

INTRODUCTION

In earthquake structural engineering, the ultimate objective is to design and build structures which are safe (against seismic loads) and economical. In order to achieve this goal in a rational manner, it is essential to have (i) a proper definition of the design ground motion, (ii) a mathematical model of the structure able to capture the essence of the non-linear hysteretic behaviour displayed by actual structures when subjected to pseudo-static cyclic loading or strong dynamic loads such as earthquake ground motions, and (iii) reliable structural damage indices based on the computed earthquake response of the mathematical structural model.

Conventional earthquake-resistant design is based on the trade-off between the yield strength of the structure and its deformation (global or local) ductility capacity. The yield strength of the structure is determined such that the deformation ductility demand imposed by the ground motion is limited to a specified target level. However, it is well-known and recognized that the deformation ductility ratio is but

* Correspondence to: J. P. Conte, Department of Civil Engineering, Rice University, P.O. Box 1892, Houston, TX 77251, U.S.A.
† Graduate student
‡ Associate Professor

Contract grant sponsor: National Science Foundation; Contract grant number: BCS-9210585

CCC 0098–8847/97/090895–22$17·50
© 1997 by John Wiley & Sons, Ltd.
Received 6 June 1996
Revised 14 January 1997

one damage parameter (or inelastic response parameter indicative of damage) and the measure of structural damage is a complex function of local and global inelastic response parameters of the structure. Thus, various damage indices have been proposed by researchers to characterize the potential level of seismic damage of a structure from the time history of its predicted inelastic response.

A general method based on inelastic response spectra to obtain preliminary seismic design forces for structures that can tolerate limited amounts of inelastic deformations has been evaluated by Mahin and Bertero.[1] A comprehensive review of the concepts and techniques used in deterministic analysis of seismic damage prediction was presented by Powell and Allahabadi.[2] McCabe and Hall[3] proposed two damage indices based on the concept of equivalent hysteretic cycles of deformation and low cycle fatigue theory. Park and Ang[4,5] defined a seismic damage index for reinforced concrete structures as a linear combination of the maximum structural deformation and the absorbed hysteretic energy, which are measures of both the largest excursion and the cumulative low-cycle fatigue types of structural damage mechanisms. By correlating analytical predictions with experimental data on cumulative damage of structural steel components subjected to cyclic inelastic loading, Krawinkler and co-workers[6,7] have assessed the prediction ability of Miner's rule and the damage assessment methodology based on low-cycle fatigue concepts and the hypothesis of linear damage accumulation which ignores load sequence effects. Chung *et al.*[8] proposed a damage index for reinforced concrete members, which combines Miner's hypothesis with damage modifiers that reflect the effects of the loading history. Equivalent ductility factors which take into account low-cycle fatigue effects are considered by Fajfar.[9] Rodriguez[10] proposed a method to reduce a multi-storey building of regular shape into an equivalent non-linear SDOF system, from which the damage indices defined for inelastic SDOF systems can be extended to characterize the overall seismic damage of multi-storey buildings. Park *et al.*[11] defined a global structural damage parameter as a weighted average of the hysteretic energies dissipated over the various structural members. Another damage evaluation procedure was developed by Shen and Soong,[12] which consists of transforming a MDOF structural system into an equivalent inelastic SDOF system and using a SDOF damage model. More recently a state-of-the-art review of seismic damage indices for concrete structures was presented by Williams and Sexsmith.[13]

This study investigates the statistics of various SDOF inelastic response parameters as functions of structural parameters and under the condition of constant-ductility design. An analytical, non-stationary earthquake ground motion model is used which is able to capture the temporal variation of both the intensity and frequency content typical of actual earthquake accelerograms. This earthquake model was recently developed by Conte and Peng[14] and is based on the theory of sigma-oscillatory processes.[15] The present study also serves as a validation, at the inelastic SDOF structural response level, of this new stochastic ground motion model calibrated for two actual earthquake accelerograms. The reason for this model validation is to ensure that the stochastic ground motion model used in this study is able to faithfully reproduce the multifold characteristics of actual earthquake ground motions. Several inelastic response parameters indicative of structural damage are considered. To study the influence of the type of hysteretic behaviour of the structure on the statistics of the structural response parameters, four different SDOF hysteretic models are considered. The mean (ensemble-average) inelastic response (or damage) spectra corresponding to various inelastic response parameters and conditioned on a fixed displacement ductility demand are computed using Monte Carlo simulation. A parametric study is carried out to determine the effects of the hysteretic model, the structural strain-hardening ratio, the target displacement ductility demand, and the ground motion process on the unconditional and conditional statistics of the inelastic response or damage spectra.

STOCHASTIC EARTHQUAKE GROUND MOTION MODEL

The non-stationary stochastic ground motion model used here is defined as a sum of zero-mean, independent, uniformly modulated Gaussian processes, $X_k(t)$. Each uniformly modulated process consists of the

 © 1997 by John Wiley & Sons, Ltd.

product of a deterministic time modulating function, $A_k(t)$, and a stationary Gaussian process, $S_k(t)$. Thus, this earthquake model is a particular sigma-oscillatory Gaussian process expressed as

$$\ddot{U}_g(t) = \sum_{k=1}^{p} X_k(t) = \sum_{k=1}^{p} A_k(t)\, S_k(t) \tag{1}$$

where $\ddot{U}_g(t)$ denotes the ground acceleration process. Furthermore, the modified gamma function is used as time modulating function, namely

$$A_k(t) = \alpha_k (t - \zeta_k)^{\beta_k} e^{-\gamma_k (t-\zeta_k)} H(t - \zeta_k) \tag{2}$$

in which α_k and γ_k are positive constants, β_k is a positive integer, ζ_k represents the 'arrival time' of the kth sub-process, $X_k(t)$, and $H(t)$ denotes the unit step function. The kth zero-mean, stationary Gaussian process, $S_k(t)$, is defined by its autocorrelation function

$$R_{S_k S_k}(\tau) = e^{-\nu_k |\tau|} \cos(\eta_k \tau) \tag{3}$$

or power spectral density function

$$\Phi_{S_k S_k}(\omega) = \frac{\nu_k}{2\pi} \left[\frac{1}{\nu_k^2 + (\omega + \eta_k)^2} + \frac{1}{\nu_k^2 + (\omega - \eta_k)^2} \right] \tag{4}$$

in which ν_k and η_k are two free parameters representing the frequency bandwidth and predominant (or central) frequency of the process $S_k(t)$, respectively. The stationary processes, $\{S_k(t),\ k = 1, 2, \ldots, p\}$, are normalized in order to have unit variance. It can be shown that the mean square function of the ground acceleration process is given by

$$E[|\ddot{U}_g(t)|^2] = \int_{-\infty}^{\infty} \sum_{k=1}^{p} |A_k(t)|^2\, \Phi_{S_k S_k}(\omega)\, d\omega = \sum_{k=1}^{p} |A_k(t)|^2 \tag{5}$$

where

$$\int_{-\infty}^{\infty} \Phi_{S_k S_k}(\omega) d\omega = R_{S_k S_k}(\tau)|_{\tau = 0} = E[|S_k(t)^2|] = 1 \tag{6}$$

and the evolutionary power spectral density function of $\ddot{U}_g(t)$ takes the form[15,16]

$$\Phi_{\ddot{U}_g \ddot{U}_g}(t, \omega) = \sum_{k=1}^{p} |A_k(t)|^2\, \Phi_{S_k S_k}(\omega) \tag{7}$$

The evolutionary (or time-varying) power spectral density function describes simultaneously the time-varying intensity, referred to as amplitude non-stationarity, and the time-varying frequency content, referred to as frequency non-stationarity. Note that the ground acceleration process, $\ddot{U}_g(t)$, is not separable although its component processes are individually separable (i.e., uniformly modulated). Each uniformly modulated component process, $X_k(t)$, is characterized by a unimodal power-spectral density function in the frequency domain and a unimodal mean square function in the time domain. Therefore, each component process captures the complex time–frequency distribution of the earthquake ground acceleration in a local time–frequency region and this ground motion model is able to reproduce the intensity and frequency non-stationary characteristics exhibited by actual earthquake accelerograms.

ESTIMATION OF MODEL PARAMETERS

The model identification and parameter estimation procedures are described in detail by the authors in a previous paper.[14] The parameters of the earthquake ground acceleration model, $\ddot{U}_g(t)$, defined above are estimated such that the analytical evolutionary power spectral density function, $\Phi_{\ddot{U}_g \ddot{U}_g}(t, \omega)$, given in equation

© 1997 by John Wiley & Sons, Ltd.

(7) best fits, in the least-squares sense, the estimated evolutionary PSD function of the target earthquake accelerogram. The latter is obtained using the short-time Thomson's multiple-window spectral estimation method.[17]

The estimated evolutionary PSD function consists of the discrete set of spectral values $\{\hat{\Phi}_{\ddot{U}_g\ddot{U}_g}[t_i, \omega_j], i = 1, 2, \ldots, N_t; j = 1, 2, \ldots, N_\omega\}$. From equations (2), (4) and (7), it follows that the analytical evolutionary power spectrum is a function of the parameter vector $\mathbf{\Theta} = [\theta_1, \theta_2, \ldots, \theta_{6p}]^T$ whose components are $(\alpha_k, \beta_k, \gamma_k, \zeta_k, \nu_k, \eta_k, k = 1, 2, \ldots, p\}$. The error or objective function is defined as

$$J(\mathbf{\Theta}) = \frac{1}{2} \sum_{i=1}^{N_t} \sum_{j=1}^{N_\omega} [\Phi_{\ddot{U}_g\ddot{U}_g}(t_i, \omega_j, \mathbf{\Theta}) - \hat{\Phi}_{\ddot{U}_g\ddot{U}_g}(t_i, \omega_j)]^2 \tag{8}$$

and is minimized with respect to the parameters $\mathbf{\Theta}$ which are subjected to simple bound constraints, i.e., all the parameters must be positive except for ζ_k. The existence of explicit closed-form solutions for the time-varying PSD and correlation functions of the response of linear elastic structures excited by the above earthquake model requires the β_k parameters to be integer-valued.[18]

NON-LINEAR HYSTERETIC MODELS

Consider the equation of motion of a non-linear hysteretic SDOF system subjected to ground excitation,

$$m\ddot{u}(t) + c\dot{u}(t) + R(t) = -m\ddot{u}_g(t) \tag{9}$$

in which m, c, $u(t)$, $R(t)$, and $\ddot{u}_g(t)$ are the system's mass, viscous damping coefficient, relative displacement with respect to the ground, non-linear restoring force, and ground acceleration, respectively. It is convenient to rewrite equation (9) in the normalized form

$$\ddot{u}(t) + 2\xi_0\omega_0\dot{u}(t) + \frac{R(t)}{m} = -\ddot{u}_g(t) \tag{10}$$

where

$$\omega_0 = \sqrt{k_0/m} \quad \text{and} \quad \xi_0 = c/(2m\omega_0) \tag{11}$$

denote the initial natural circular frequency and initial damping ratio corresponding to the unyielded system (k_0 is the initial or pre-yield stiffness). The viscous damping coefficient c is assumed to be constant (independent of the system inelastic behaviour), which is a typical assumption in non-linear structural dynamic analysis.

Four different hysteretic models are considered to represent a variety of non-linear restoring force properties of the structure, namely the bilinear hysteretic model, a modified version of the original stiffness degrading model proposed by Clough and Johnston,[19] the slip model defined by Tanabashi and Kaneta,[20] and the curvilinear (smooth) Bouc–Wen model first proposed by Bouc,[21] and later generalized by Wen,[22] Park *et al.*[11] and others. These four hysteretic models are shown in Figure 1. Each of the inelastic SDOF structures considered in this study is completely defined by the following structural parameters:

(1) initial (or pre-yield) natural period: $T_0 = 2\pi/\omega_0$ (sec);
(2) initial damping ratio: $\xi_0 = c/(2\sqrt{k_0 m})$, dimensionless;
(3) strength coefficient, $\eta = R_y/(\text{mg})$, dimensionless, in which R_y and $U_y = R_y/k_0$ represent the structure's yield strength and yield displacement, respectively, and g denotes the acceleration of gravity;
(4) strain hardening ratio: $\alpha = k_p/k_0$, the dimensionless ratio of the post-yield stiffness, k_p, to the pre-yield stiffness, k_0.

The stable, non-degrading, bilinear hysteretic model, Figure 1(a), is often used to represent the restoring force characteristics of steel moment-resisting frames in the absence of local buckling. Clough's stiffness degrading model accounts for the effect of stiffness degradation in R/C moment-resisting frames caused by

 © 1997 by John Wiley & Sons, Ltd.

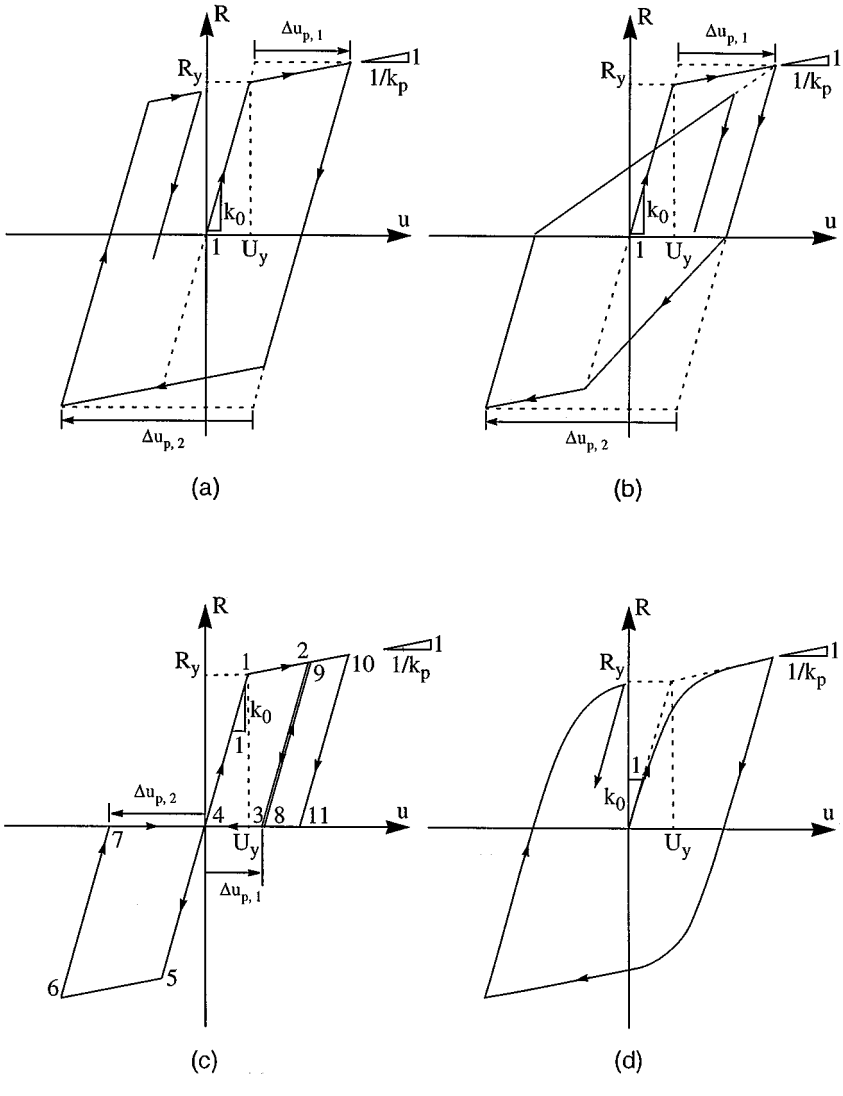

Figure 1. Nonlinear hysteretic restoring force models: (a) bilinear model; (b) Clough's stiffness degrading model; (c) slip model; (d) Bouc–Wen model

load reversals in the inelastic range. This model is also representative of R/C shear wall behaviour dominated by flexural deformations. The slip model approximates the behaviour of steel-braced frames having a significant brace buckling effect and also the behaviour of R/C members in which shear distortion or bond-slip action dominates the overall behaviour. The Bouc–Wen model, because of its convenient mathematical form, has been widely used in non-linear probabilistic structural dynamics.[21,22] The force–deformation relationship, $R(t)$ versus $u(t)$, of the Bouc–Wen model is expressed through a state variable, $z(t)$, which is governed by a non-linear differential equation, namely,

$$R(t) = \alpha k u(t) + (1 - \alpha) k z(t) \tag{12}$$

$$\dot{z}(t) = \frac{A\dot{u}(t) - v[\beta|\dot{u}(t)||z(t)|^{n-1} z(t) + \gamma\dot{u}(t)|z(t)|^n]}{\rho} \tag{13}$$

© 1997 by John Wiley & Sons, Ltd.

where, if $A = 1$, α and k correspond to the previously defined strain hardening ratio and pre-yield stiffness k_0, respectively, and the coefficients A, β, γ, v, ρ and n are 'loop parameters' controlling the shape and magnitude of the hysteresis loop and the smoothness of the transition from the elastic to the inelastic region. By assigning appropriate values to these parameters, this hysteretic model can describe a wide range of softening and hardening systems. It can be shown that the Bouc–Wen model tends to the bilinear inelastic model as the parameter n becomes large. Although stiffness and strength degradations can be incorporated into the Bouc–Wen model as functions of the total hysteretic energy dissipation and maximum response of the system, only the stable, non-deteriorating version of the model is considered here. For a unit value of the parameter A, the yield strength R_y of the Bouc–Wen model, see Figure 1(d), can be obtained as

$$R_y = k_0 U_y \quad \text{where} \quad U_y = \left[\frac{1}{(\gamma + \beta)v}\right]^{1/n} \tag{14}$$

The following parameter values defined the Bouc–Wen model used in this study: $A = \rho = 1$, $n = 2$, $\gamma = \beta = 0{\cdot}5$.

ENERGY AND POWER BALANCE EQUATION

The energy balance equation is obtained by integrating the equation of motion, equation (9), with respect to the relative displacement response, u. Thus,

$$\int_{u(0)}^{u(t)} m\ddot{u}\,\mathrm{d}u + \int_{u(0)}^{u(t)} c\dot{u}\,\mathrm{d}u + \int_{u(0)}^{u(t)} R\,\mathrm{d}u = -\int_{u(0)}^{u(t)} m\ddot{u}_g\,\mathrm{d}u \tag{15}$$

Using the relation $\mathrm{d}u = \dot{u}\mathrm{d}\tau$, the above equation can be written as

$$\int_0^t m\ddot{u}(\tau)\dot{u}(\tau)\,\mathrm{d}\tau + \int_0^t c\dot{u}^2(\tau)\,\mathrm{d}\tau + \int_0^t R(\tau)\dot{u}(\tau)\,\mathrm{d}\tau = -\int_0^t m\ddot{u}_g(\tau)\dot{u}(\tau)\,\mathrm{d}u \tag{16}$$

or, more succinctly,

$$E_K(t) + E_D(t) + E_S(t) = E_I(t) \tag{17}$$

where $E_K(t) = \frac{1}{2}m\dot{u}^2(t) - \frac{1}{2}m\dot{u}^2(0)$ is the kinetic energy, $E_D(t)$ is the energy dissipated through viscous damping up to time t, $E_S(t)$ is the total energy absorbed by the spring which is composed of the recoverable elastic strain energy, $E_E(t)$, and the permanently dissipated hysteretic energy, $E_H(t)$, and $E_I(t)$ denotes the earthquake input energy.

The power balance equation is simply obtained by differentiating the energy balance equation with respect to time,

$$\frac{\mathrm{d}E_K(t)}{\mathrm{d}t} + \frac{\mathrm{d}E_D(t)}{\mathrm{d}t} + \frac{\mathrm{d}E_S(t)}{\mathrm{d}t} = \frac{\mathrm{d}E_I(t)}{\mathrm{d}t} \tag{18}$$

or, from equations (16) and (17),

$$m\ddot{u}(t)\dot{u}(t) + c\dot{u}^2(t) + R(t)\dot{u}(t) = -m\ddot{u}_g(t)\dot{u}(t) \tag{19}$$

© 1997 by John Wiley & Sons, Ltd.

NON-LINEAR INELASTIC STRUCTURAL RESPONSE PARAMETERS

The various non-linear inelastic structural response parameters considered in the present study are defined below.

(a) maximum displacement ductility:

$$\mu_d = \underset{0 \leqslant t \leqslant t_d}{\text{Max}} \, |u(t)/U_y|$$

(t_d denotes the ground motion duration)

(b) number of yield reversals: n_{rev};

(c) maximum normalized plastic deformation range:

$$\left(\frac{\Delta u_{p,i}}{U_y}\right)_{max} = \underset{0 \leqslant t \leqslant t_d}{\text{Max}} \left|\frac{\Delta u_{p,i}}{U_y}\right|$$

(see Figure 1 for definition of the plastic deformation range $\Delta u_{p,i}$)

(d) normalized cumulative displacement ductility:

$$\mu_{acc} = \left(\sum_{i=1}^{N} |\Delta u_{p,i}|/U_y\right) + 1$$

(e) residual displacement ductility:

$$\mu_{res} = |u_{res}|/U_y,$$

where u_{res} represents the permanent deformation (shift) of the structure at the end of the ground motion excitation;

(f) normalized earthquake input energy:

$$E_I = \left[\int_0^{t_d} dE_I(t)\right] \Big/ (R_y U_y)$$

(g) normalized total hysteretic energy dissipated:

$$E_H = \left[\int_0^{t_d} dE_H(t)\right] \Big/ (R_y U_y)$$

(h) ratio of total hysteretic energy dissipated to earthquake input energy: E_H/E_I

(i) maximum rate of normalized earthquake input energy:

$$P_{I,max} = \underset{0 \leqslant t \leqslant t_d}{\text{Max}} \left[\frac{1}{R_y U_y} \frac{dE_I(t)}{dt}\right]$$

(j) maximum rate of normalized energy dissipated through viscous damping:

$$P_{D,max} = \underset{0 \leqslant t \leqslant t_d}{\text{Max}} \left[\frac{1}{R_y U_y} \frac{dE_D(t)}{dt}\right]$$

(k) maximum rate of normalized hysteretic energy dissipated:

$$P_{H,max} = \underset{0 \leqslant t \leqslant t_d}{\text{Max}} \left[\frac{1}{R_y U_y} \frac{dE_H(t)}{dt}\right]$$

The last three response parameters are indicative of how fast the earthquake input energy is imparted to and dissipated by the structure. These power response quantities must be related to the extent and type of seismic damage inflicted to the structure by the ground motion. For a given total amount of hysteretic energy dissipated, a low and uniform rate and a highly variable, spiky rate of hysteretic energy dissipation must correspond to different levels and types of structural damage.

© 1997 by John Wiley & Sons, Ltd.

APPLICATION EXAMPLES AND EARTHQUAKE MODEL VALIDATION

Earthquake model identification and artificial ground motion simulation

The stochastic earthquake ground motion model described above is applied to two actual earthquake ground acceleration records (accelerograms) having very different non-stationarity characteristics. The first record corresponds to the S00E (N–S) component of the Imperial Valley earthquake of May 18, 1940, recorded at El Centrosite and shown in Figure 4(b). The second record consists of the N00W (N–S) component of the San Fernando earthquake of February 9, 1971, recorded at Orion Blvd. site and displayed in Figure 4(e).

Figures 2 and 3 contain the analytical time-varying PSD function, $\Phi_{\ddot{U}_g\ddot{U}_g}(t, \omega)$, of the identified non-stationary earthquake model for the 1940 El Centro target record, and the 1971 Orion Blvd. target record,

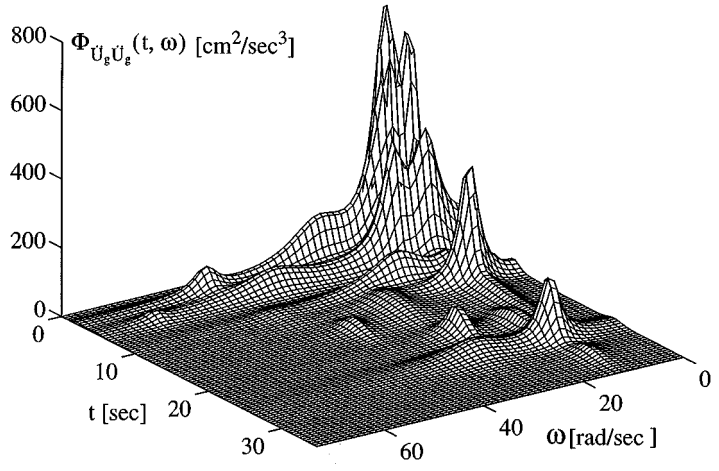

Figure 2. Analytical time-varying PSD function of the identified earthquake model for the 1940 El Centro target record

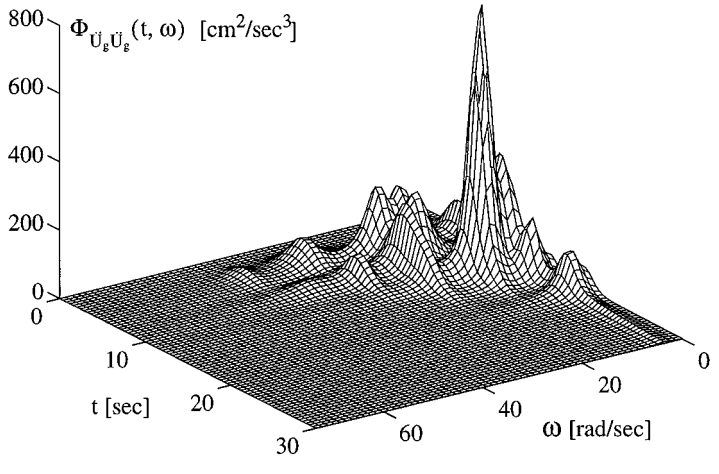

Figure 3. Analytical time-varying PSD function of the identified earthquake model for the 1971 Orion Blvd. Target record

© 1997 by John Wiley & Sons, Ltd.

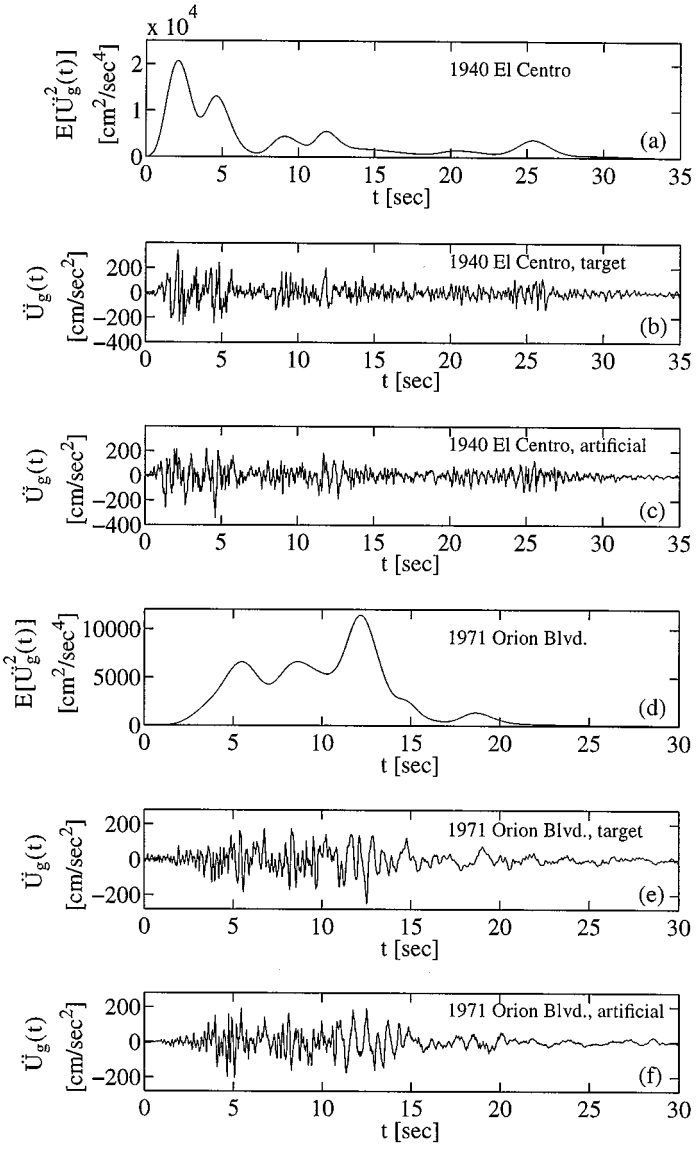

Figure 4. Mean-square functions of underlying ground acceleration process and target and artificial ground acceleration time histories

respectively. These time-varying PSD functions show the temporal variation of the frequency content of the underlying ground acceleration process. Typically, the frequency content shifts progressively towards the low-frequency range as time progresses. A single realization of the identified stochastic earthquake model for each of the two target records is given in Figures 4(c) and 4(f). Notice that these artificial ground acceleration time histories are substantially similar to the respective target accelerogram. The mean square ground acceleration functions of the two identified earthquake models are plotted in Figures 4(a) and 4(d).

A sample of 100 artificial accelerograms is simulated from each of the identified earthquake models to evaluate the model's ability to faithfully reproduce the multifold characteristics of the target earthquake ground motion. For each ground motion realization, the component processes are simulated independently

© 1997 by John Wiley & Sons, Ltd.

using the spectral representation method,[23] time-modulated, and added to form an artificial ground acceleration record. Then the artificial ground motions are baseline-corrected in the frequency domain by using a simple rectangular high-pass filter with a cut-off frequency at 0.10 Hz and by applying a least-squares straight-line fitting to both the integrated ground velocity and displacement records.

First level of earthquake model validation

For the two target earthquake accelerograms considered here, the first level of model validation was presented in a previous paper.[14] It consisted of comparing the first- and second-order statistics of traditional ground motion parameters and the probabilistic linear-elastic response spectra obtained through Monte Carlo simulation of the earthquake model with their deterministic counterparts characterizing the target record.

Second level of earthquake model validation

The second level of earthquake model validation involves comparing various probabilistic inelastic response spectra with their (deterministic) target counterpart. These probabilistic inelastic response spectra are also estimated from the sample of 100 artificial earthquake ground motions used in the first level of model validation. The probabilistic inelastic response spectra are characterized by their mean, mean $\pm$ one standard deviation, and 5 and 95 per cent fractiles. For the purpose of gaining insight into the statistical implications of constant-ductility design, the so-called probabilistic constant-ductility response spectra are introduced. For each of the 100 artificial ground motions and for each nonlinear inelastic SDOF system considered, the strength level $R_y = \eta(\text{mg})$ corresponding to a specified displacement ductility demand μ_d is computed iteratively. Thus, this inverse iterative calculation provides a set of 100 strength coefficients for each inelastic SDOF and for each level of displacement ductility demand considered. These strength coefficients are then used to compute various probabilistic inelastic response spectra conditioned on specified levels of displacement ductility demand (for *each* artificial ground motion realization). These conditioned probabilistic inelastic response spectra are called herein *probabilistic constant-ductility response spectra* and are defined for any inelastic response parameter of interest. The estimated mean (sample mean) of the probabilistic constant-ductility response spectra are referred to as *ensemble-average constant-ductility response spectra* in the sequel. The unconditioned probabilistic inelastic response spectra considered below correspond to a fixed strength level (across all ground motion realizations and for a given initial period of the SDOF system) given by the ensemble-average constant-ductility strength coefficient spectrum (for a specified displacement ductility demand). The second level of earthquake model validation is based on these unconditioned probabilistic inelastic response spectra.

The inelastic restoring force behaviour of the SDOF structures is modelled by the four non-linear hysteretic models described earlier. An initial damping ratio of 5 per cent is used throughout the study. Strain-hardening ratios of 0 and 5 per cent and an initial undamped structural period ranging from 0·1 to 3·0 sec are considered. A comprehensive parametric study is performed by varying the target ground motion (i.e., the stochastic ground motion model), the hysteretic SDOF structural model, and the structural parameters. Only a selective and representative set of these results is displayed below, but the discussion of the results reflects the whole parametric study.

Probabilistic constant-ductility strength coefficient spectra for a target displacement ductility demand $\mu_d = 6$ are shown in Figure 5 for the four non-linear hysteretic restoring force models and for both the 1940 El Centro and 1971 Orion Blvd. stochastic earthquake models. The deterministic constant-ductility strength coefficient spectra obtained directly from the target earthquake ground motions are also represented (in solid line) in Figure 5. Because the displacement ductility criterion addresses only the single maximum response occurring over a number of deformation cycles, the yield strength must be adjusted to control this single response value, and thereby causing the deterministic spectral shape to become distorted and uneven.[24] On

 © 1997 by John Wiley & Sons, Ltd.

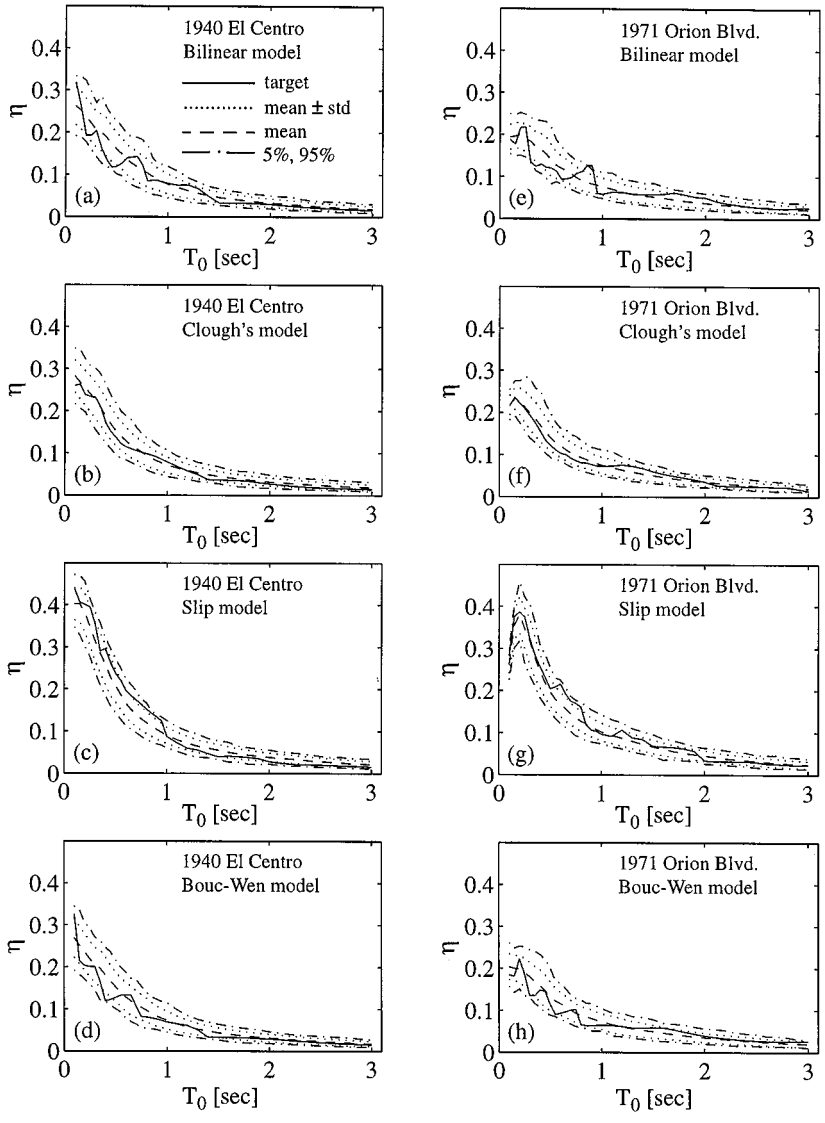

Figure 5. Probabilistic constant-ductility strength coefficient spectra ($\alpha = 0$ per cent, $\xi_0 = 5$ per cent, $\mu_d = 6$)

the other hand, the various fractiles of the probabilistic spectra are quite smooth in shape reflecting the fact that they originate from the stochastic ground motion model and not from a single realization thereof as in the deterministic case. The probabilistic response spectra have the advantage of being risk-consistent along the initial structural period axis, which is not the case of the deterministic spectra. Risk-consistent inelastic response spectra represent very useful tools for reliability-based earthquake-resistant design. It is observed that for both earthquake models (El Centro and Orion Blvd.), the target strength coefficient spectrum is contained within the 'mean $\pm$ one standard deviation' interval in the case of Clough's stiffness degrading model. For the other restoring force models considered, the target strength coefficient spectrum falls between the 5 and 95 per cent fractiles of the corresponding probabilistic spectrum.

© 1997 by John Wiley & Sons, Ltd.

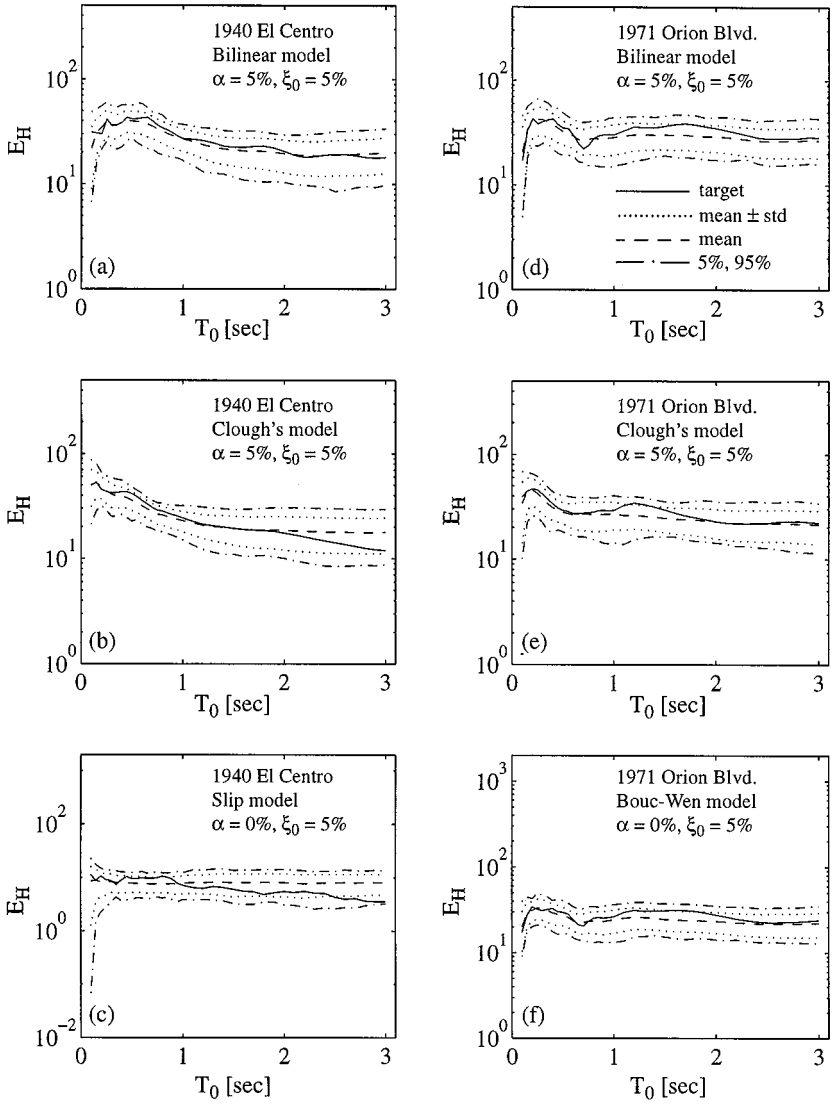

Figure 6. Probabilistic normalized total hysteretic energy dissipated response spectra ($\eta = \hat{E}[\eta]$ for $\mu_d = 6$ as shown in Figures 5 and 8)

Figure 6 shows the probabilistic normalized total hysteretic energy dissipated response spectra for a yield strength given by the ensemble-average (or sample mean) of the yield strengths required for a constant displacement ductility demand of $\mu_d = 6$ as shown in Figures 5 and 8. The normalized total hysteretic energy dissipated has been widely recognized for being an important response parameter indicative of the cumulative damage imparted to structures by earthquake excitations. Therefore, this response parameter plays an important role in seismic damage assessment studies of structures. It is essential that the stochastic earthquake model captures well this damage index as predicted from the target earthquake ground motion. As shown in Figure 6, the target normalized total hysteretic energy dissipated response spectra fall almost entirely within the 'mean $\pm$ one standard deviation' interval and are always well contained between the 5 and 95 per cent fractiles of the corresponding probabilistic spectra.

 © 1997 by John Wiley & Sons, Ltd.

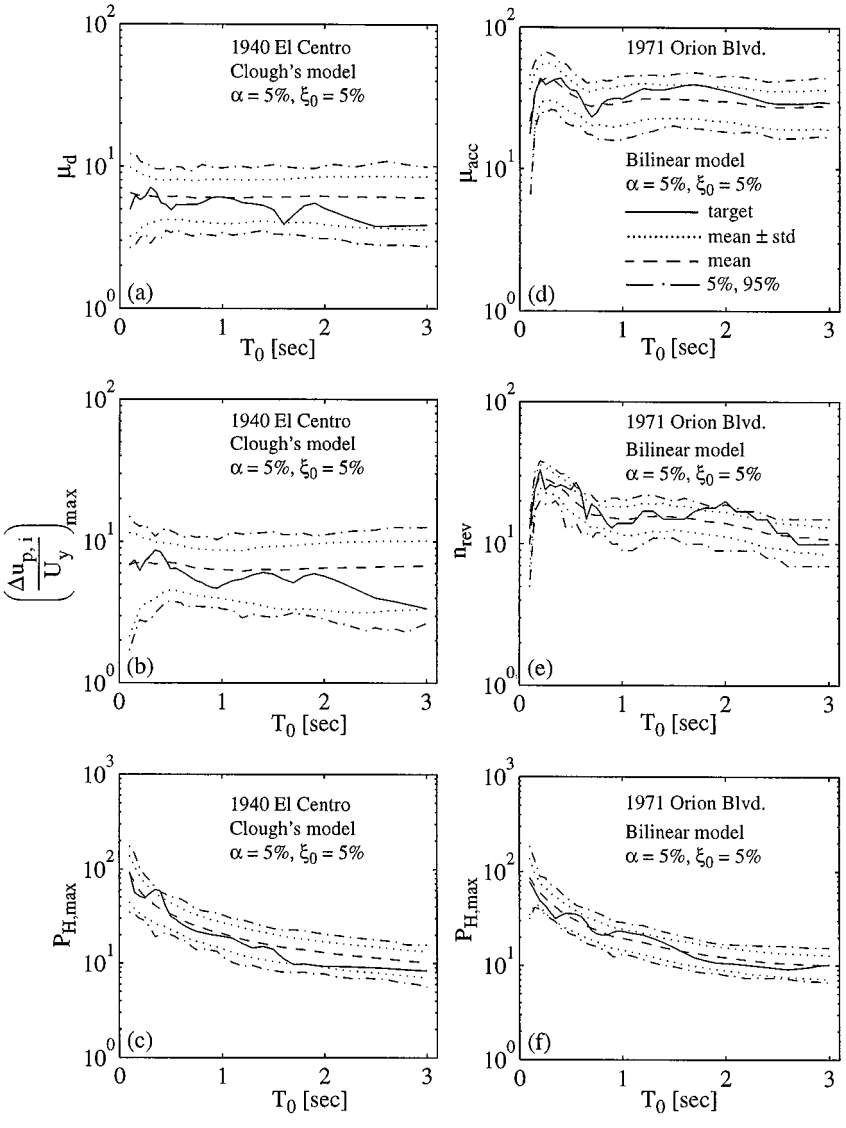

Figure 7. Probabilistic inelastic response spectra ($\eta = \hat{E}[\eta]$ for $\mu_d = 6$ as shown in Figure 8)

Another significant damage parameter is the maximum displacement ductility μ_d[4,25,26] whose target and probabilistic spectra are given in Figure 7(a) for the El Centro earthquake model. Notice that the mean ductility response spectrum is almost constant at the value $\mu_d = 6$. This is the target ductility demand used in determining the ensemble-average yield strength on which the probabilistic ductility response spectra in Figure 7(a) is based. It is observed that the target displacement ductility response spectrum falls within the 'mean $\pm$ one standard deviation' statistical range of the corresponding probabilistic spectrum.

Other probabilistic inelastic response spectra for the Clough's stiffness degrading and the bilinear hysteretic models are given in Figures 7(b)–7(f) for both the 1940 El Centro and 1971 Orion Blvd. earthquake

© 1997 by John Wiley & Sons, Ltd.

models. All the target inelastic response spectra shown in Figure 7 fall almost entirely within the 'mean $\pm$ one standard deviation' interval of their probabilistic counterpart and are well contained between the 5 and 95 per cent fractiles. This statistical consistency between the target and probabilistic inelastic response spectra validates, at the inelastic structural response level, the non-stationary earthquake model used in this study. In other words, this stochastic earthquake model is able to capture all the ground motion features to which inelastic structures are significantly sensitive.

INELASTIC RESPONSE SPECTRA CONDITIONED ON CONSTANT DISPLACEMENT DUCTILITY DEMAND

Conventional earthquake-resistant design consists in determining the yield strength R_y (or yield strength coefficient η) required to limit the displacement ductility demand, μ_d, imposed by the design ground motion to a specified level which depends on the structural material and lateral load resisting system used. Thus, constant-ductility strength coefficient spectra are the proper design tools and were first introduced by Veletsos and Newmark.[25,26] Although the maximum displacement ductility response represents an important index to estimate earthquake-induced structural damage, it is well recognized that a structure can be damaged or weakened by a combination of stress reversals in the inelastic range and high stress excursion.[4] The final part of this study investigates the statistics of various inelastic response (or damage) parameters conditioned on constant displacement ductility demand for the four hysteretic models and two earthquake processes defined above. The effect of the strain-hardening ratio on these conditional statistics is also examined.

Yield strength coefficient demand

The ensemble-average (or sample mean denoted by $\hat{E}[\ \ldots\ ]$) constant-ductility strength coefficient spectra for $\mu_d = 1$, 2, 3 and 6 are shown in Figure 8 for both the El Centro and Orion Blvd. stochastic earthquake models and for the bilinear, Clough's, and slip hysteretic models. The spectra in solid line correspond to the strain-hardening ratio $\alpha = 0$ per cent, while those in dotted line correspond to the strain-hardening ratio $\alpha = 5$ per cent. As expected, the ensemble-average strength coefficient is very sensitive to the target displacement ductility demand μ_d and to the initial structural period in the low period range ($T_0 < 1{\cdot}0$ sec). It is observed that a 5 per cent strain-hardening ratio has very little effect on the ensemble-average strength coefficient spectra for low target ductility levels or for higher initial structural periods. As the target ductility demand increases, the influence of the strain-hardening ratio on the required yield strength increases in the low initial period range for both earthquake models and for all four hysteretic models considered. The bilinear inelastic model is more sensitive to the effect of the strain-hardening ratio than the other restoring force models. Notice the similarity in shape of the ensemble-average strength coefficient spectra for different restoring force models and different earthquake processes.

Strength reduction factor

The strength reduction factor, R_{μ_d}, is defined as the ratio of the elastic strength demand to the yield strength required to limit the maximum displacement ductility demand at the specified value μ_d. Note that the elastic strength demand corresponds to the yield strength required to limit the maximum displacement ductility demand at $\mu_d = 1$, or equivalently to keep the SDOF structure in the elastic range. A comprehensive evaluation of the strength reduction factor for earthquake-resistant design is given by Miranda and Bertero.[27] The ensemble-average constant-ductility strength reduction factor spectra are shown in Figure 9 for the El Centro and Orion Blvd. earthquake models and for the bilinear, Clough's, and slip hysteretic models. The strength reduction factor spectra in solid lines and dotted lines correspond to the

 © 1997 by John Wiley & Sons, Ltd.

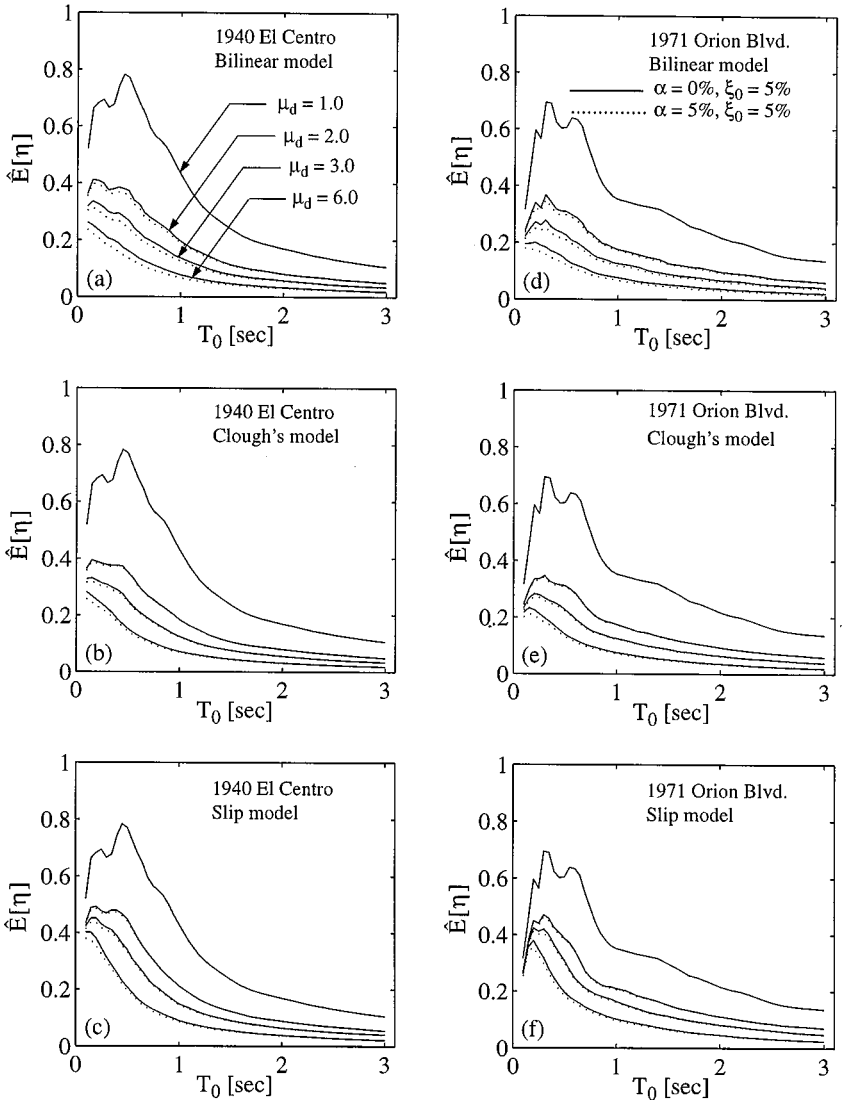

Figure 8. Ensemble-average constant-ductility strength coefficient spectra

strain-hardening ratio $\alpha = 0$ per cent and $\alpha = 5$ per cent, respectively. As in the case of the strength coefficient, the effect of a positive strain-hardening ratio on the ensemble-average strength reduction factor spectra increases as the target ductility demand increases, especially for the bilinear inelastic model. The ensemble-average strength reduction factor spectra generally increase to almost a constant level as the initial structural period T_0 increases, except in the case of the Orion Blvd. earthquake model for a relatively high ductility demand of $\mu_d = 6$. In summary, the ensemble-average strength reduction factor (i) depends strongly on the initial structural period in the low period range and the target displacement ductility demand, (ii) depends moderately on the target earthquake ground motion and the type of hysteretic model, and (iii) depends weakly on the strain-hardening ratio.

© 1997 by John Wiley & Sons, Ltd.

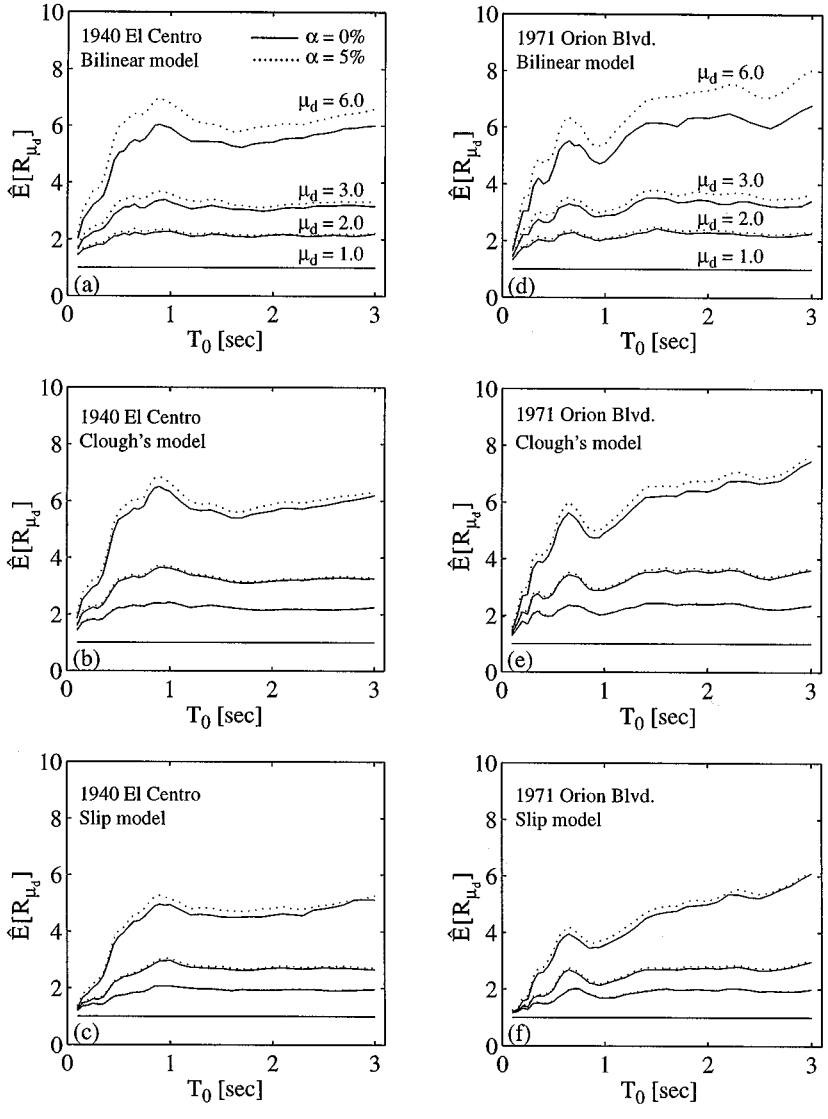

Figure 9. Ensemble-average constant-ductility reduction factor spectra ($\xi_0 = 5$ per cent)

Normalized total hysteretic energy dissipated

The normalized total hysteretic energy dissipated, E_H is an important inelastic response parameter used in the definition of most seismic damage indices.[10,11,24,28,29] The ensemble-average constant-ductility normalized total hysteretic energy dissipated spectra corresponding to $\mu_d = 6$ only are shown in Figure 10 for the 1940 El Centro earthquake model and for the bilinear, Clough's slip, and Bouc–Wen hysteretic models. The following observations are made concerning the effects of the earthquake ground motion process, the target maximum displacement ductility demand μ_d, and the structural properties (type of hysteretic behaviour, initial period, and strain-hardening ratio) on the ensemble-average constant-ductility

 © 1997 by John Wiley & Sons, Ltd.

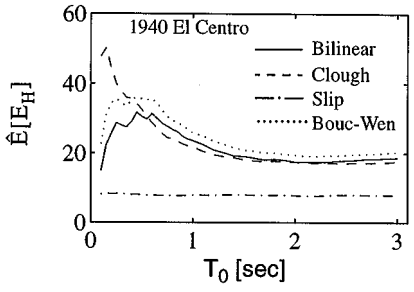

Figure 10. Ensemble-average normalized total hysteretic energy dissipated response spectra ($\mu_d = 6$, $\xi_0 = 5$ per cent, $\alpha = 0$ per cent)

normalized total hysteretic energy dissipated, $\hat{E}[E_H]$.

(i) The ensemble-average constant-ductility E_H spectrum increases with the maximum displacement ductility demand μ_d as expected.
(ii) The ensemble-average constant-ductility E_H spectrum is sensitive to the type of hysteretic behaviour of the structure, especially in the low initial period range.
(iii) The results obtained for the effect of the hysteretic model on the ensemble-average of the normalized total hysteretic energy dissipated are consistent with those of Loh and Ho.[28] Accordingly, non-linear hysteretic models can be classified into three groups regarding the prediction of E_H, namely the bilinear, modified Clough's, and slip model groups.
(iv) For the slip hysteretic model, the ensemble-average constant-ductility E_H spectra are not sensitive to the initial period of the structure and are almost constant for a specified maximum displacement ductility demand.
(v) The effect of the strain-hardening ratio, α, on the ensemble-average constant-ductility E_H spectra becomes significant as the maximum displacement ductility demand μ_d increases and can amount to a 40 per cent increase for the bilinear hysteretic model and an initial period between 0·4 and 0·5 sec. The bilinear model is more sensitive to the strain-hardening ratio than the other hysteretic models considered.
(vi) The shapes of the ensemble-average constant-ductility E_H spectra remain very similar for the El Centro and Orion Blvd. earthquake processes.

Other inelastic response or damage parameters

The ensemble-average constant-ductility response spectra corresponding to other inelastic response or damage parameters are given in Figure 11 for the bilinear hysteretic model only and for several values of target displacement ductility μ_d. The inelastic response or damage parameters include the number of yield reversals, n_{rev}, the maximum normalized plastic deformation range, $(\Delta u_{p,i}/U_y)_{max}$, the residual displacement ductility, μ_{res}, and the ratio of total hysteretic energy dissipated to earthquake input energy, E_H/E_I. The four hysteretic models considered are compared in Figure 12 for the target ductility level $\mu_d = 6$ only. The important effects of the earthquake process, the target displacement ductility demand μ_d, the initial structural period, and the strain-hardening ratio on these ensemble-average constant-ductility response spectra are summarized below.

(a) The ensemble-average constant-ductility E_H/E_I spectra increase significantly with the maximum displacement ductility demand μ_d. This property is consistent with the deterministic results obtained by Zahrah and Hall.[24] As shown in Figures 11(a) and 11(e), the proportion of the earthquake input energy dissipated by hysteretic yielding is sensitive to the initial period of the structure in the low

© 1997 by John Wiley & Sons, Ltd.

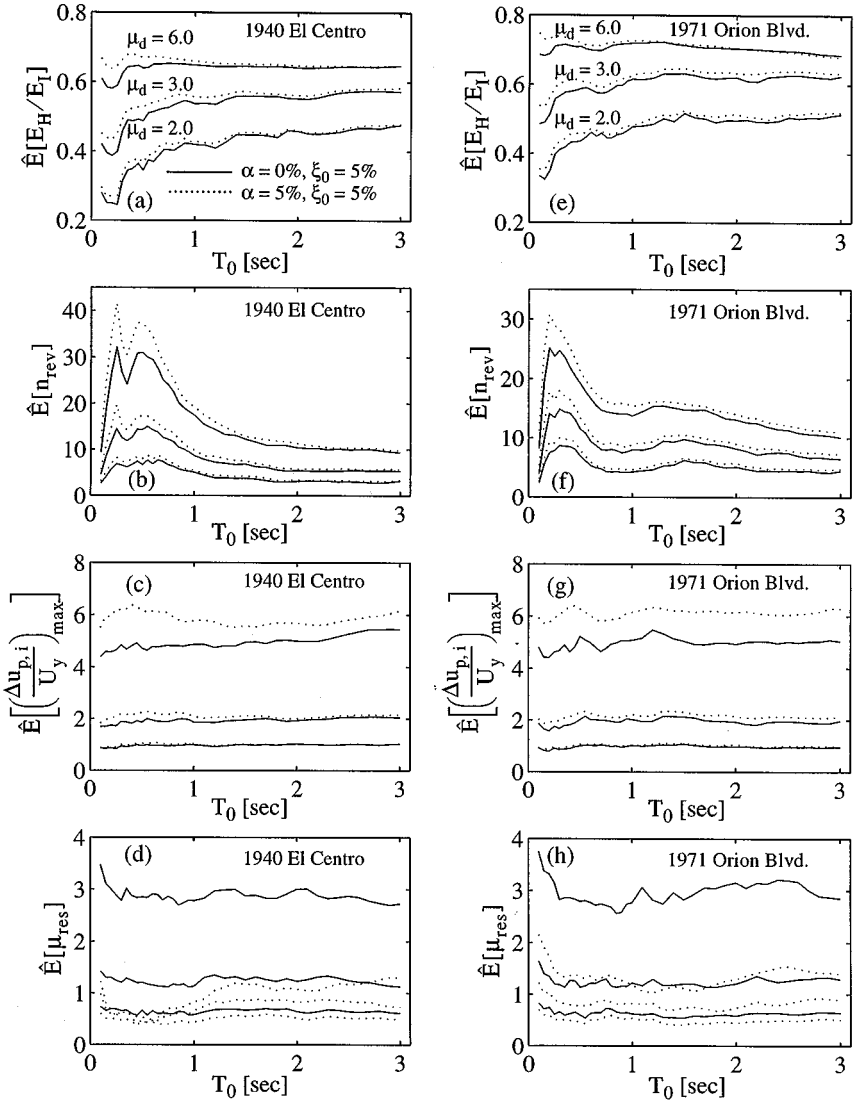

Figure 11. Ensemble-average constant-ductility response spectra for bilinear hysteretic model

period range only ($T_0 < 1{\cdot}0$ sec). For higher initial structural periods, the ensemble-average E_H/E_I spectra are almost constant. It is also observed that the ensemble-average E_H/E_I spectra are sensitive to the earthquake process: for a given ductility demand μ_d, the ratio E_H/E_I is systematically higher for the Orion Blvd. than for the El Centro earthquake process.

(b) Similarly, the ensemble-average constant-ductility n_{rev}, $(\Delta u_{p,i}/U_y)_{max}$ and μ_{res} spectra increase significantly with the ductility demand μ_d. The ensemble-average n_{rev} spectra are highly sensitive to the initial structural period T_0 in the range $T_0 < 1{\cdot}0$ sec and become almost constant for higher initial periods. The ensemble-average $(\Delta u_{p,i}/U_y)_{max}$ and μ_{res} spectra are very insensitive to the initial structural period.

(c) As the strain-hardening ratio, α, increases from 0 to 5 per cent, the ensemble-average constant-ductility response spectra for E_H/E_I, n_{rev}, and $(\Delta u_{p,i}/U_y)_{max}$ increase, especially in the low initial period range.

 © 1997 by John Wiley & Sons, Ltd.

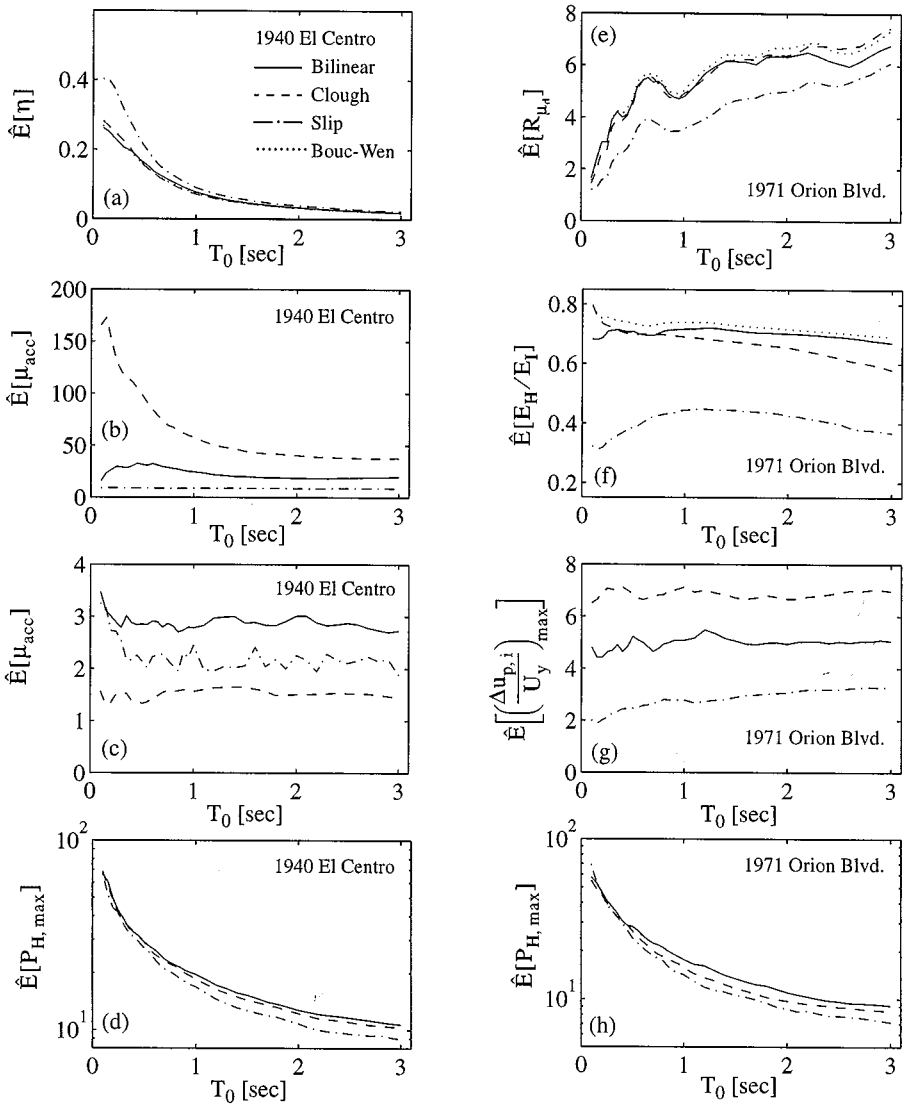

Figure 12. Ensemble-average constant-ductility response spectra ($\mu_d = 6$, $\xi_0 = 5$ per cent, $\alpha = 0$ per cent)

On the other hand, the ensemble-average constant-ductility μ_{res} spectra decrease tremendously as α increases. This is consistent with previous deterministic studies which have shown that a positive, even small, strain-hardening ratio has a strong 'centering effect' on the earthquake response of inelastic structures.

(d) The ensemble-average constant-ductility response spectra corresponding to E_H/E_I, n_{rev}, $(\Delta u_{p,i}/U_y)_{max}$, and μ_{res} for the El Centro earthquake model are very similar in shape and magnitude (except for E_H/E_I) to those for the Orion Blvd. earthquake model.

(e) Since the ensemble-average constant-ductility inelastic response spectra corresponding to important damage parameters such as μ_{acc}, n_{rev}, E_H, and $P_{H,max}$ are not constant over the initial structural period axis, *constant ductility design* does not ensure *constant-damage design*, which is a more desirable design criterion.

© 1997 by John Wiley & Sons, Ltd.

Comparison between different hysteretic models

For a constant-ductility demand of $\mu_d = 6$, the ensemble-average response spectra corresponding to various inelastic response parameters and to the four hysteretic models considered in this study are displayed in Figure 12 for both the El Centro and Orion Blvd. earthquake models. The following observations are made.

(1) As shown in Figure 12(a) for a constant ductility demand $\mu_d = 6$, the ensemble-average strength coefficient spectra, $\hat{E}[\eta]$, are larger for the slip model than for the other hysteretic models. This difference between the slip and other hysteretic models is particularly large in the low initial period range ($T_0 < 1{\cdot}0$ sec). This implies that the design yield strength for a given constant ductility demand is larger for the slip model than for the other hysteretic models. This is also manifested in the ensemble-average constant-ductility strength reduction factor spectra which are lower for the slip model than for the other hysteretic models, see Figure 12(e). Because of its higher strength requirement for a constant ductility demand μ_d, and its poor hysteretic energy dissipation capacity (pinched hysteresis loop, see Figure 1(c)), the slip hysteretic model produces ensemble-average constant-ductility response spectra for E_H, μ_{acc}, E_H/E_I, $(\Delta u_{p,i}/U_y)_{max}$, and $P_{H,max}$, which are significantly lower than for the other three hysteretic models considered here.
(2) The ensemble-average constant-ductility E_H spectrum is largest for Clough's model in the initial structural period range between 0·1 and 0·3 sec, and it is largest for the Bouc–Wen model in the initial period range higher than 0·4 sec. In this regard, it should be recalled that from their definition, Clough's stiffness degrading and Bouc–Wen models continuously dissipate hysteretic energy after first yield has occurred, which is not the case for the bilinear and slip hysteretic models. The same trend can be observed from the ensemble-average constant-ductility E_H/E_I spectra in Figure 12(f).
(3) The ensemble-average of the ratio of total hysteretic energy dissipated to earthquake input energy, $\hat{E}[E_H/E_I]$, depends on the hysteretic model and the initial structural period, especially in the low period range. The slip model always exhibits the lowest $\hat{E}[E_H/E_I]$ spectrum, while Clough's model produces the highest $\hat{E}[E_H/E_I]$ spectrum for initially very stiff structures. For moderate and high initial structural periods, the Bouc–Wen model gives the highest $\hat{E}[E_H/E_I]$ spectrum.
(4) The ensemble-average constant-ductility response spectra for μ_{acc}, $(\Delta u_{p,i}/U_y)_{max}$, μ_{res}, and $P_{H,max}$ are strongly dependent on the hysteretic model over the whole initial period range from 0·1 to 3·0 sec. Clough's model gives the largest $\hat{E}[\mu_{acc}]$ and $\hat{E}[(\Delta u_{p,i}/U_y)_{max}]$ spectra, while the corresponding lowest ensemble-average spectra are produced by the slip hysteretic model.

CONCLUSIONS

As the first objective of this study, a recently developed stochastic earthquake ground motion model non-stationary in both intensity and frequency content is validated at the inelastic SDOF structural response level. This validation is based on two identified earthquake models corresponding to the N–S components of the 1940 El Centro and 1971 Orion Blvd. earthquake records. Four nonlinear hysteretic SDOF restoring force models are used, namely the bilinear, modified Clough's stiffness degrading, slip, and Bouc–Wen models. Various inelastic response parameters based on (i) force–deformation response quantities, (ii) energy response quantities, and (iii) rate of energy (power) response quantities are considered. Statistics (mean, mean $\pm$ one standard deviation, 5 and 95 per cent fractiles) of the probabilistic inelastic response spectra are obtained using Monte Carlo simulation. They are based on a sample of one hundred artificial earthquake ground motions simulated from the El Centro and Orion Blvd. identified stochastic earthquake models. The estimated probabilistic inelastic response spectra are found statistically consistent with the deterministic inelastic response spectra obtained directly from the target earthquake ground motion records, which validates the stochastic earthquake ground motion model at the level of inelastic SDOF structural response. In other words, this statistical consistency (i.e., deterministic spectra mostly contained between the 5 and 95 per cent fractiles of the corresponding probabilistic spectra) signifies that the target earthquake record can be

 © 1997 by John Wiley & Sons, Ltd.

regarded as a single member of the family of infinitely many artificial earthquake records defined by the identified stochastic earthquake ground motion model.

As the second and main objective of this study, the design criterion of constant maximum displacement ductility demand used in conventional earthquake-resistant design is examined from the statistical viewpoint using the two identified stochastic earthquake models. This study investigates the effects of the earthquake process, the type of hysteretic behaviour, the initial structural period T_0, the strain-hardening ratio, and the target maximum displacement ductility demand μ_d on the ensemble-average of the probabilistic inelastic response spectra conditioned on specified levels of μ_d (called ensemble-average constant-ductility response spectra) and corresponding to various inelastic response parameters indicative of damage. The most salient results of this statistical parametric study are summarized below.

(1) The ensemble-average constant-ductility response spectra are generally highly dependent on the initial period of the structure in the low period range ($T_0 < 1{\cdot}0$ sec). The ensemble-average of the inelastic response parameters are generally higher in this low initial period range than in the higher initial period range. It is also found that in this low initial period range, the ensemble-average constant-ductility response spectra are very sensitive to the type of hysteretic behaviour. The above trends are clearly observed in the case of the number of yield reversals, n_{rev}, the normalized cumulative displacement ductility, μ_{acc}, the normalized total hysteretic energy dissipated, E_H, and the ratio of total hysteretic energy dissipated to earthquake input energy, E_H/E_I.
(2) A positive strain-hardening ratio has little effect on the ensemble-average constant-ductility strength coefficient spectra. However, it can have significant effects on the various inelastic response or damage spectra, especially in the low initial period range and for the bilinear hysteretic model.
(3) It is traditionally believed[27] that the strength reduction factor is not significantly dependent on the hysteretic model. However, the ensemble-average constant-ductility response spectra for various inelastic response parameters can be very sensitive to the hysteretic model. The relative effects of different hysteretic models should be recognized in earthquake-resistant design and the hysteretic model should be selected carefully accounting for the actual properties of the structural system and structural materials at hand.
(4) The overall shapes of the various ensemble-average constant-ductility response spectra remain similar for the two identified earthquake models considered in this study.
(5) The methodology used in this study is very useful in producing risk-consistent strength coefficient design spectra for constant ductility design.
(6) Since the ensemble-average constant-ductility inelastic response spectra corresponding to important damage parameters such as μ_{acc}, n_{rev}, E_H, and $P_{H,max}$ are not constant over the initial structural period axis, *constant ductility design* does not ensure *constant-damage design*, which is a more desirable, but more difficult to formulate and implement, design criterion.

Ensemble-average response spectra obtained from an ensemble of actual earthquake ground motions[27] tend to be smooth in shape as the probabilistic response spectra analyzed in this study. However, they are not risk-consistent as their shape depends on the relative scaling of the actual accelerograms, an operation which remains somewhat arbitrary[30]. Relative scaling is usually performed based on an agreed upon damage index (defined as either a ground motion parameter or an elastic or inelastic SDOF structural response parameter) characterizing ground motion intensity. However, it was found[30] that no single known damage index is able to characterize consistently the damage potential of strong earthquake ground motions. The probabilistic (risk-consistent) spectra defined here are conditioned on a single earthquake source and magnitude. In the more realistic case of multiple potential earthquake sources, unconditional probabilistic (risk-consistent) spectra would be obtained by integrating the conditional probabilistic spectra over the continuum range of possible magnitude and over all the possible sources accounting for the probability distribution of the earthquake magnitude and the earthquake risk associated with each source (i.e., by using the total

© 1997 by John Wiley & Sons, Ltd.

probability theorem). In summary, the probabilistic approach provides the rational framework to derive risk-consistent response spectra, which the deterministic approach does not offer.

A comprehensive study of the sensitivity of the various probabilistic constant-ductility response spectra on the ground motion process would require the use of a large number of actual earthquake records (more than the two used herein) from each of which an earthquake ground motion process would be calibrated. However, this was out of the scope of the present study.

ACKNOWLEDGEMENTS

Support from the National Science Foundation under Grant No. BCS-9210585, with Dr. Shih-Chi Liu as Program Director, is gratefully acknowledged. The constructive comments of the reviewers are greatly appreciated.

REFERENCES

1. S. A. Mahin and V. V. Bertero, 'An evaluation of inelastic seismic design spectra', *J. struct. div. ASCE* **107**, 1777–1795 (1981).
2. G. H. Powell and R. Allahabadi, 'Seismic damage prediction by deterministic methods: concepts and procedures', *Earthquake Engng. Struct. Dyn.* **16**, 719–734 (1988).
3. S. L. McCabe and W. J. Hall, 'Assessment of seismic structural damage', *J. struct. eng. ASCE* **115**, 2166–2183 (1989).
4. Y.-J. Park and A. H.-S. Ang, 'Mechanistic seismic damage model for reinforced concrete', *J. struct. eng. ASCE* **111**, 722–739 (1985).
5. Y.-J. Park and A. H.-S. Ang and Y.-K. Wen, 'Seismic damage analysis of reinforced concrete buildings', *J. struct. eng. ASCE* **111**, 722–739 (1985).
6. H. Krawinkler and M. Zohrei, 'Cumulative damage in steel structures subjected to earthquake ground motions', *Comput. structures* **16**, 531–541 (1983).
7. H. Krawinkler, 'Performance assessment of steel components', *Earthquake spectra* **3**, 27–41 (1987).
8. Y. S. Chung, C. Meyer and M. Shinozuka, 'Modeling of concrete damage', *ACI struct. J.* **86**, 259–271 (1989).
9. P. Fajfar, 'Equivalent ductility factors, taking into account low-cycle fatigue', *Earthquake Engng. Struct. Dyn.* **21**, 837–848 (1992).
10. M. Rodriguez, 'A measure of the capacity of earthquake ground motions to damage structures', *Earthquake Engng. Struct. Dyn.* **23**, 627–643 (1994).
11. Y. J. Park, A. H.-S. Ang and Y.-K. Wen, 'Damage-limiting aseismic design of buildings', *Earthquake spectra* **3**, 1–26 (1987).
12. K. L. Shen and T. T. Soong, 'Seismic damage evaluation of multi-story structures', in *Computational Stochastic Mechanics*, Balkema, Rotterdam, 1995. pp. 249–257.
13. M. S. Williams and R. G. Sexsmith, 'Seismic damage indices for concrete structures: a state-of-the-art review', *Earthquake spectra* **11**, 319–349 (1995).
14. J. P. Conte and B.-F. Peng, 'Fully nonstationary analytical earthquake ground motion model', *J. eng. mech. ASCE* **123**, 15–24 (1997).
15. F. Battaglia, 'Some extensions in the evolutionary spectral analysis of a stochastic process', *Bolletino dell' Unione Matematica Italiana* **16B**, 1154–1166 (1979).
16. M. B. Priestley, *Spectral Analysis and Time Series*, Academic Press, New York, 1987.
17. D. J. Thomson, 'Spectrum estimation and harmonic analysis', *Proc. IEEE* **70**, 1055–1096 (1982).
18. J. P. Conte and B.-F. Peng, 'An explicit closed-form solution for linear systems subjected to nonstationary random excitation', *Prob. eng. mech.* **11** (1), 37–50, (1996).
19. R. W. Clough and S. B. Johnston, 'Effect of stiffness degradation on earthquake ductility requirements', *Proc. 2nd Japan nat. conf. earthquake eng.*, 1966, pp. 227–232.
20. R. Tanabashi and K. Kaneta, 'On the relation between the restoring force characteristics of structures and pattern of the earthquake ground motions', *Proc. Japan nat. symp. earthquake eng.*, Tokyo, 1962, pp. 57–62.
21. R. Bouc, 'Forced vibration of mechanical system with hysteresis, abstract', *Proc. 4th conf. nonlinear oscillation*, Prague, Czechoslovakia, 1967.
22. Y.-K. Wen, 'Method for random vibration of hysteretic systems', *J. eng. mech. div. ASCE* **102**, 249–263 (1976).
23. M. Shinozuka and C. M. Jan, 'Digital simulation of random processes and its applications', *J. sound vib.* **25**, 111–128 (1972).
24. T. F. Zahrah and W. J. Hall, 'Earthquake energy absorption in SDOF structures', *J. eng. mech. div. ASCE* **110**, 1757–1772 (1984).
25. A. S. Veletsos and N. M. Newmark, 'Effect of inelastic behavior on the response of simple systems to earthquake ground motions', *Proc. 2nd world conf. earthquake eng.*, Japan 1960, Vol. II, pp. 895–912.
26. A. S. Veletsos, N. M. Newmark and C. V. Chelapati, 'Deformation spectra for elastic and elastoplastic systems subjected to ground shock and earthquake motion', *Proc. 3rd world conf. earthquake eng.*, New Zealand, 1965, Vol. II, pp. 663–682.
27. E. Miranda and V. V. Bertero, 'Evaluation of strength reduction factors for earthquake-resistant design', *Earthquake spectra* **10**, 357–379 (1994).
28. C.-H. Loh and R.-C. Ho, 'Seismic damage assessment based on different hysteretic rules', *Earthquake Engng. Struct. Dyn.* **19**, 753–771 (1990).
29. J. Osteraas and H. Krawinkler, 'The Mexico earthquake of September 19, 1985—behavior of steel buildings', *Earthquake spectra* **5**, 51–87 (1994).
30. J. Lin and S. A. Mahin, 'Effect of Inelastic Behavior on the Analysis and Design of Earthquake Resistant Structures', *UCB/EERC 85/08*, Earthquake Engineering Research Center, University of California, Berkeley, CA, 1985.

 © 1997 by John Wiley & Sons, Ltd.